ARTICLE OPEN

Check for updates

Soluble form of Lingo2, an autism spectrum disorder-associated molecule, functions as an excitatory synapse organizer in neurons

Fumiaki Yoshida[1], Ryota Nagatomo[1], Shun Utsunomiya[2], Misaki Kimura[1], Shiyori Shun[1], Rena Kono[3], Yuma Kato[1], Yosuke Nao[1], Kazuma Maeda[2], Ryuta Koyama[3,4,5], Yuji Ikegaya[3,4,6], Stefan F. Lichtenthaler[7,8,9], Sho Takatori[1], Hiroshi Takemoto[2,10], Koichi Ogawa[2], Genta Ito[11,12] and Taisuke Tomita[1,12]✉

Autism Spectrum Disorder (ASD) is a developmental disorder characterized by impaired social communication and repetitive behaviors. In recent years, a pharmacological mouse model of ASD involving maternal administration of valproic acid (VPA) has become widely used. Newborn pups in this model show an abnormal balance between excitatory and inhibitory (E/I) signaling in neurons and exhibit ASD-like behavior. However, the molecular basis of this model and its implications for the pathogenesis of ASD in humans remain unknown. Using quantitative secretome analysis, we found that the level of leucine-rich repeat and immunoglobulin domain-containing protein 2 (Lingo2) was upregulated in the conditioned medium of VPA model neurons. This upregulation was associated with excitatory synaptic organizer activity. The secreted form of the extracellular domain of Lingo2 (sLingo2) is produced by the transmembrane metalloprotease ADAM10 through proteolytic processing. sLingo2 was found to induce the formation of excitatory synapses in both mouse and human neurons, and treatment with sLingo2 resulted in an increased frequency of miniature excitatory postsynaptic currents in human neurons. These findings suggest that sLingo2 is an excitatory synapse organizer involved in ASD, and further understanding of the mechanisms by which sLingo2 induces excitatory synaptogenesis is expected to advance our understanding of the pathogenesis of ASD.

Translational Psychiatry (2024)14:448 ; https://doi.org/10.1038/s41398-024-03167-5

INTRODUCTION

Autism Spectrum Disorder (ASD) is a neurodevelopmental disorder that typically begins in childhood. The DSM-5, the most widely used diagnostic tool for ASD, defines it as a broad concept that includes impairments in social communication and the presence of restricted and repetitive activities and interests. The number of individuals diagnosed with ASD is increasing, with an estimated prevalence of 1–2% [1–7]. Despite this, the underlying causes of ASD are not yet understood and there are no established diagnostic methods or pharmacological treatments based on the underlying pathogenesis.

The balance between excitatory and inhibitory synapses, known as the excitatory/inhibitory (E/I) balance, has been proposed to be important for normal brain development and function. This idea is supported by evidence that E/I balance is disrupted in several brain disorders, including ASD [8]. For example, 10-30% of individuals with ASD experience epilepsy caused by the excessive synchronized firing of neurons, and a reduction in GABAergic signaling has been observed in individuals with ASD [9, 10]. In addition, research using optogenetics has shown that stimulation of excitatory neurons in the prefrontal cortex, thought to be involved in social behavior, decreases sociality, whereas stimulation of inhibitory neurons does not alter sociality in mice [11]. This strongly supports the E/I balance hypothesis that disruption of the E/I balance in an excitatory-dominant state leads to ASD-like behavior.

Valproic acid (VPA) is a commonly used antiepileptic and mood-stabilizing drug [12]. VPA affects the activity of GABAergic inhibitory neurons and regulates gene expression by inhibiting histone deacetylase (HDAC) [13]. A Danish study found that exposure to VPA during pregnancy increased the risk of developing ASD [14]. A prospective 11-year study showed that VPA monotherapy as well as the use of multiple drugs

[1]Laboratory of Neuropathology and Neuroscience, Graduate School of Pharmaceutical Sciences, The University of Tokyo, Tokyo, Japan. [2]Neuroscience 2, Laboratory for Drug Discovery and Disease Research, Shionogi & Co. Ltd, Osaka, Japan. [3]Laboratory of Chemical Pharmacology, Graduate School of Pharmaceutical Sciences, The University of Tokyo, Tokyo, Japan. [4]Institute for AI and Beyond, The University of Tokyo, Tokyo, Japan. [5]5Department of Translational Neurobiology, National Institute of Neuroscience, National Center of Neurology and Psychiatry, Tokyo, Japan. [6]Center for Information and Neural Networks, National Institute of Information and Communications Technology, Osaka, Japan. [7]German Center for Neurodegenerative Diseases (DZNE), Munich, Germany. [8]Neuroproteomics, School of Medicine, Klinikum rechts der Isar, Technical University of Munich, Munich, Germany. [9]Munich Cluster for Systems Neurology (SyNergy), Munich, Germany. [10]Business-Academia Collaborative Laboratory (Shionogi), Graduate School of Pharmaceutical Science, The University of Tokyo, Tokyo, Japan. [11]Department of Biomolecular Chemistry, Faculty of Pharma-Science, Teikyo University, Tokyo, Japan. [12]Social Cooperation Program of Brain and Neurological Disorders, Graduate School of Pharmaceutical Sciences, The University of Tokyo, Tokyo, Japan.
✉email: taisuke@mol.f.u-tokyo.ac.jp

Received: 28 September 2024 Revised: 13 October 2024 Accepted: 15 October 2024
Published online: 23 October 2024

including VPA increased the prevalence of neurodevelopmental disorders [15]. Studies in rodents have also examined the effects of maternal exposure to VPA and observed symptoms of ASD, such as impaired social communication and repetitive behaviors [16–20]. While in the general population autism is four times more common in males than in females, the prevalence of autism in children exposed to VPA during pregnancy is characterized by an even (1:1) male to female ratio [21]. Similarly, in rodents, maternal challenge with VPA induces autistic-like phenotypes in both male and female offspring [20]. Electrophysiological studies have shown that the density of NMDA receptors in neocortical regions is increased in VPA-treated rats, resulting in enhanced long-term potentiation (LTP) [22]. Electrophysiological studies have also shown that maternal VPA treatment increases the frequency and amplitude of miniature excitatory postsynaptic currents (mEPSCs) in the amygdala [23]. In the prefrontal cortex, an increase in excitatory synapses, as well as activated microglia and activated astrocytes have been observed [24]. In addition, at the molecular level, the expression of excitatory synaptic-related molecules such as PSD-95, α-CaMKII, and vGlut1 is increased [25, 26].

Synapse formation and synaptic remodeling are critical for the formation of accurate neural circuits during development and throughout life [27]. Synapse organizer proteins, including cell adhesion molecules such as Neuroligin and Neurexin, and secreted proteins such as Hevin, play a role in synapse formation [28, 29]. Neuroligin binds to neurexin at the presynapse to induce synapse formation, while secreted factors such as FGF22 and FGF7 have been reported to induce excitatory and inhibitory synapses, respectively [30]. Recent research has shown that synaptic organizer proteins are more strongly correlated with the development of ASD [31].

We identified the novel excitatory synapse organizer protein, Lingo2, from the culture supernatant of primary cultured neurons in the valproic acid (VPA) maternal administration ASD model mouse. We demonstrated that Lingo2 is cleaved by ADAM10, resulting in the secretion of soluble Lingo2, and that this soluble Lingo2 induces abnormalities in excitatory synapse formation not only in mouse primary cultured neurons but also in excitatory neurons derived from human iPSCs. Hence, soluble Lingo2 might serve as a potential therapeutic target for ASD.

MATERIAL AND METHOD

Cell culture, biochemical, and molecular biological experiments were performed as previously described [32–39]. All methods were performed in accordance with the relevant guidelines and regulations. Detailed protocols for antibodies, compounds, and immunological methods are described in the Supplementary Information.

Animal

The animal care and use procedures were approved by the Institutional Animal Care and Use Committee/ethics committee of the Graduate School of Pharmaceutical Sciences, The University of Tokyo (protocol no. P29-31). Mice for primary cultures were purchased from SLC (Japan). Prenatal VPA exposure has performed as previously described [25]. Briefly, pregnant ICR mice were purchased from Japan SLC, Inc. VPA (SIGMA) was suspended in 0.9% saline. The dosage was 600 mg/kg and adjusted according to the body weight of the dam on the day of injection. Treated dams received a single subcutaneous injection on gestational day 13 (embryonic 13 days) and control dams received a single injection of saline. Those dams were housed individually and allowed to raise their litters. The offspring were used for experiments on indicated timing. Both male and female mice were used in the experiment.

Generation of iPSC-derived neural cells

Studies with human Ngn2 knock-in (KI) iPSCs were approved by the Ethics Committee on Human Tissues and Genome Research at Shionogi & Co., Ltd. (approval number KS17-027, KS18-016, KS19-023 and The University of Tokyo/Office for Life Science Research Ethics and Safety. Feeder-free 201B7 human iPSCs were purchased from iPS Academia Japan Inc [40, 41]. Ngn2 Knock-In iPSCs were generated as previously described [42]. Differentiation of iPSCs to neural progenitors (NPs) and neurons in adherent culture was performed as previously described with slight modification [37]. Briefly, on day 0, confluent iPSCs were passaged onto Matrigel-coated dishes and cultured in AK03N medium (Ajinomoto). On day 1, doxycycline was added to the medium to induce the expression of Ngn2. On day 2, an equal volume of N2 medium was added to the AK03N medium, and N2 Medium was used on days 3-4. On day 5, an equal amount of NB medium was added to the N2 medium, and NB medium was used on days 6-8. From day 5, cytosine arabinoside (AraC) was added to the medium to inhibit the proliferation of NPs. N2 medium contains DMEM/F12, 1X N2 supplement (Invitrogen). 1X NEAA (Invitrogen), mouse laminin (0.20 µg/ml), NT-3 (10 ng/ml), and BDNF (10 ng/ml). NB medium contains Neurobasal, 1X B-27 supplement (Invitrogen), 1X GlutaMAX-1 supplement (Invitrogen), mouse laminin (0.2 µg/ml), NT-3 (10 ng/ml), and BDNF (10 ng/ml). From day 11, Brainphys Neuronal Medium and SM1 supplement (Stem Cell Technology) was used to promote further neural maturation.

Secretome Protein enrichment with click sugars (SPECS)

Metabolic labeling and purification of Azido sugar-labeled proteins were conducted as previously described [43, 44] with slight modification. In brief, 10 million neurons were plated. After four DIV, neurobasal medium was exchanged for neurobasal medium supplemented with 50 µM tetraacetyl-N-azidoacetyl mannosamine (ManNAZ). After two days, conditioned media were collected, filtered through a 0.45 µm PVDF Millex filter (Millipore, Darmstadt, Germany), and concentrated using a VivaSpin 20 centrifugal concentrator (30 kDa) at 4 °C. Non-metabolized ManNAZ was removed from the VivaSpin 20 columns by centrifugation at 5000 *g* at 4 °C. The retentate was rinsed with 20 ml ddH2O three times. In the final step, we added 100 µM of DBCO-S-S-PEG3-Biotin and 0.2% formic acid diluted in 500 µl ddH2O to the retentate to biotinylate the metabolically azide-labeled glycoproteins. Columns were incubated overnight at 4 °C. Non-reactive DBCO-S-S-PEG3-Biotin was removed by filling the retentate with 20 ml of pH 7.5 Tris buffer and centrifuged at 5000 x *g* at 4 °C. The Vivaspin 20–30 k columns were centrifuged twice and the retentate was diluted in 20 ml of ddH2O. Finally, the retentate was diluted in 5 ml of 2% SDS in PBS after the last centrifugation.

In-gel digestion and LC-MS/MS analysis

The SPECS experiments were performed after treatment with or without valproic acid each in triplicate, and proteins biotinylated in SPECS experiments were pulled down using Streptavidin Sepharose High Performance (GE Healthcare) and eluted by heating the beads in 1× LDS Sample Buffer (Thermo Fisher Scientific) containing 2.5% (v/v) 2-mercaptoethanol at 70 degrees for 10 min.

The samples were run on a Bolt 4–12% Bis-Tris Plus gel (Thermo Fisher Scientific) until the dye front reaches the center of the gel. The gel was stained with a Colloidal Blue Staining Kit (Thermo Fisher Scientific) and subjected to in-gel digestion followed by an LC-MS/MS analysis (Medical ProteoScope, Inc., Japan). In-gel digestion was performed as described previously [45]. Briefly, a region from the top of the gel to the top of the albumin band and a region from the bottom of the albumin band to the 25 kDa marker were cut out. The gel slices were further dissected into 1-mm square cubes and destained in water. The gel pieces were treated with dithiothreitol and iodoacetamide for carbamidomethylation of

cysteine residues and then digested with trypsin for 16 h at 37 degrees. The tryptic peptides were extracted from the gel pieces and dried down.

The dried peptides were resolubilized in solvent A (water: acetonitrile: trifluoroacetic acid (TFA) = 98: 2: 0.1 by volume). The one-fourth of the samples were purified on a nano HPLC column (particle size: 3 µm; inner diameter: 100 µm; length: 15 cm) (L-column Micro; Chemical Evaluation and Research Institute, Japan), at a constant flow rate of 500 nL/min, with a gradient 5–35% B in 100 min; solvent A: water/acetonitrile/formic acid 98:2:0.1 (v:v:v); solvent B: water/acetonitrile/formic acid 10:90:0.1 (v:v:v) on Paradigm MS4 (Michrom Bioresources). The MS analysis was performed on an LTQ Orbitrap XL mass spectrometer (Thermo Fisher Scientific) with the top 10 acquisition method: MS resolution 30,000, between 300 and 1500 m/z.

Raw MS data were processed using Progenesis QI for proteomics version 2.0 (Nonlinear Dynamics), and searches were performed against the Mouse SwissProt database together with a database of common contaminants provided by the Global Proteome Machine Organization (https://www.thegpm.org/crap/) on Mascot (Matrix Science). Enzyme specificity was set to semi-trypsin, up to 2 missed cleavages were allowed for protease digestion, and the search included cysteine carbamidomethylation as a fixed modification and oxidation of methionine as a variable modification. Peptide tolerance was set to +/− 5 ppm, and MS/MS tolerance was set to +/− 0.5 Da. The peptide identification was performed with a false discovery rate of 0.01. The abundance of a protein was calculated by integrating the intensity of unique peptides assigned to the protein. All identified proteins were listed in the supplementary table.

Hippocampal slice culture

To prepare slice cultures, P6 mouse brains were sectioned into 400-µm-thick horizontal slices using a DTK-1500 vibratome (Dosaka, Kyoto, Japan) in aerated, ice-cold Gey's balanced salt solution (GBSS) containing 36 mmol/L glucose, as previously described [46] Briefly, the entorhinohippocampal regions of the slices were dissected out and incubated for 60–90 minutes at 4 °C in a cold incubation medium containing minimal essential medium (MEM), 9.0 mM Tris, 22.9 mM HEPES, and 63.1 mM glucose supplemented with penicillin and streptomycin. Following incubation, the slices were placed on Omnipore membrane filters (JHWP02500; Merck Millipore, Billerica, MA, USA) on doughnut plates (Hazai-Ya, Tokyo, Japan) [47] in a solution containing 50% MEM, 25% horse serum (26050-088; HS, heat-inactivated and filter-sterilized, Gibco, Grand Island, NY, USA), 25% HBSS, 6.6 mM Tris, 16.9 mM HEPES, and 4.0 mM NaHCO3 supplemented with 29.8 mM glucose and 1% gentamicin sulfate solution (16672-04; Nacalai Tesque, Kyoto, Japan). Finally, the slices were cultured at 35 °C in a humidified incubator with 5% CO2 and 95% air. The culture medium was changed twice a week. At 6 and 7 days in vitro (DIV), 10 nM recombinant sLingo2 or PBS (5 µl per slice) was treated in a drop-wise manner.

Quantification

The percentage of excitatory and inhibitory synapses was measured in the following way. The merge area of vGlut1 and synaptophysin, the merge area of vGat and synaptophysin, and the area of synaptophysin were measured. The percentage of excitatory and inhibitory synapses was measured by dividing the merged area by the area of synaptophysin.

Excitatory synapses in hippocampal slice culture were analyzed using the following procedure. Z-series images were collected at 0.33 µm intervals. The stacked images were analyzed using ImageJ. vGlut1 channels were processed with the "Subtract background" command and thresholded using the Moments method. The puncta whose areas were bigger than 0.1 µm^2 were defined as vGlut1+ synapses. To eliminate the areas of cell soma from ROI, NeuroTrace channels were thresholded using the Huang method, and the areas with more than 2 µm^2 were calculated. The mean fluorescent intensity within each punctum besides the NeuroTrace+ area was measured using the particle analysis command and averaged per image.

Electrophysiology

Whole-cell voltage-clamp recordings were performed in iPSC-induced neuronal cells. Induced neuronal cells were transferred to a recording chamber and perfused a bath solution of HEPES buffer consisting of 130 mM NaCl, 2.5 mM KCl, 2.0 mM $CaCl_2$, 1.0 mM $MgCl_2$, 10 mM HEPES, 10 mM d-Glucose. Glass pipettes (2-5 MΩ) were filled with an intracellular solution containing the following: 130 mM K-Gluconate, 2.0 mM NaCl, 20 mM HEPES, 4.0 mM $MgCl_2$, 0.25 mM EGTA, 4.0 mM Mg-ATP, 0.4 mM GTP-Tris. The pH was 7.3 (Adjusted with KOH). For mEPSC recordings, 1.0 µM tetrodotoxin was added to the bath solution to block Na^+ currents.

Statistical analysis

All samples were analyzed in a randomized manner. No statistical methods were used for the sample size. No animal was excluded from the analysis. Experimenters were blind to drug treatments. For quantitative analyses, the student *t*-test was used for comparisons between two-group data, and the Tukey test was used for multiple-group comparisons. If other statistical methods were used, they were described in the legend. Statistical analyses were performed by Kyplot or Excel software. In the figures, statistical results were indicated by absolute *p* values. A p-value < 0.05 was considered to have a significant difference. The exact mean values, SEMs, F- and *p*-values for ANOVA, and *p*-values for post-hoc test are reported in the Supplementary Information.

RESULTS

Maternal VPA-treated primary neurons secreted the excitatory presynapse organizer

Maternal treatment with valproic acid (VPA) has been shown to result in the development of autism spectrum disorder (ASD)-like phenotypes, such as impaired social communication and repetitive behaviors, in mouse models. In these animals, alterations in the excitatory-inhibitory (E/I) ratio have been observed in electrophysiological analyses. However, the effect of maternal VPA administration on synaptogenesis in neurons is not well understood. To investigate this, we examined the protein expression levels of synapse-related molecules in primary cultured neurons derived from VPA-treated pregnant mice at 6 days in vitro (DIV6) (Fig. 1A). We found that prenatal VPA administration resulted in a marked increase in the expression of the excitatory presynaptic marker molecule vesicular glutamate transporter 1 (vGlut1), while the expression of the inhibitory presynaptic marker vesicular GABA transporter (vGat) was unchanged (Fig. 1B, C). Immunocytochemical analyses using anti-vGlut1 and vGat antibodies were used to quantify the formation of excitatory and inhibitory synapses, respectively. Consistent with the biochemical analysis, the area of vGlut1-positive puncta was significantly increased, whereas the area of vGat-positive puncta remained unchanged (Fig. 1D, E).

To identify the molecule(s) responsible for the VPA-induced increase in excitatory presynapses, we tested the synaptogenic activity of conditioned medium from primary cultured neurons of VPA-treated maternal fetuses (CM-VPA) in primary cultured neurons separately seeded from wild-type mice (Fig. 1F). CM-VPA treatment increased the expression of vGlut1 but did not alter the expression of vGat (Fig. 1G, H). Furthermore, the addition of CM-VPA increased the area of vGlut1-positive puncta (Fig. 1I, J). Notably, this increase in excitatory synaptic puncta was abolished by boiling CM-VPA, while the percentage of vGat-positive puncta

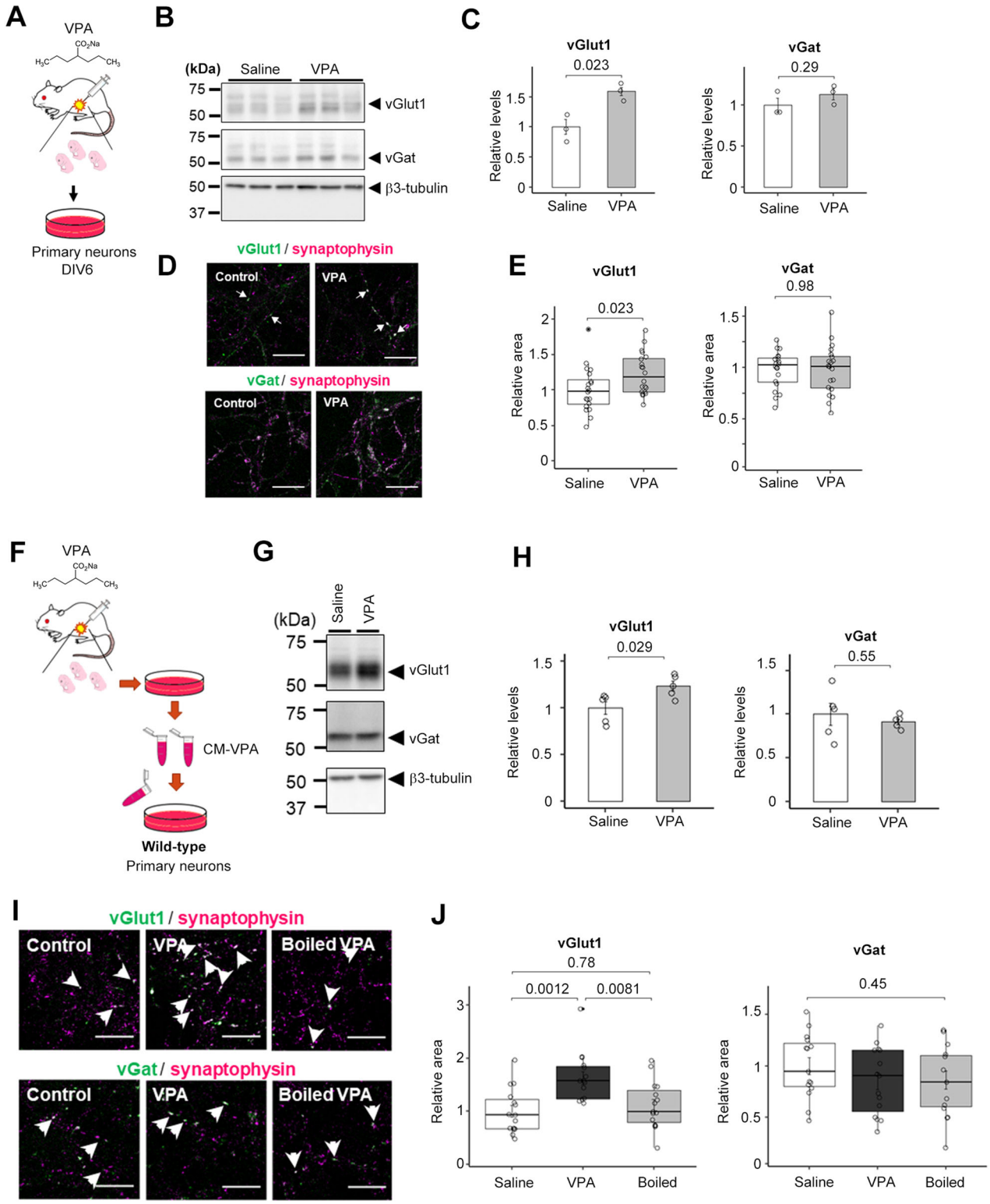

remained unchanged. These results suggest that CM-VPA contains presynaptic organizer protein(s) that enhance the formation of excitatory synapses in primary neurons.

Lingo2 expression level was increased in the VPA maternal administration model

To identify the VPA-induced synaptic organizer protein, we performed a quantitative secretome analysis using the Secretome Protein Enrichment with Click Sugars (SPECS) method, which overcomes several limitations of secretome analysis, such as the low concentration of secreted proteins and contamination by serum and cytoplasmic proteins in the culture medium [43]. After the metabolic labeling of glycans with azide-labeled sugar in living cells, newly glycosylated proteins were selectively biotinylated by a 2 + 3 cycloaddition reaction. Subsequently, biotin-labeled secreted proteins were specifically detected by the avidin-biotin

Fig. 1 Maternaly VPA-treated neurons secrete excitatory synapse-inducing factor(s). A Schematic depiction of this experiment. 600 mg/kg VPA or saline was injected by i.p. into the pregnant mouse. **B** Immunoblot analysis of relative expression levels of synaptic proteins in mouse primary neurons obtained from maternal VPA-treated pups. **C** Quantification of the relative expression levels of synaptic proteins in **B**) ($n = 3$-4, Mean ± SEM, by Student's *t*-test, n.s. indicates $P > 0.05$). Saline, saline-treated neuron; VPA, VPA-treated neuron's medium. The expression of the vGlut1 was significantly increased, but the expression of the vGat was unchanged. **D** Immunocytochemical analyses of maternal VPA-treated primary neurons stained for synaptophysin, vGat, and vGlut1. Scale bar = 10 µm. **E** Quantification of vGlut1- and vGat-positive presynapse areas in **D** ($n = 20$, Mean ± SEM, by Student's *t*-test, n.s. indicates $P > 0.05$). The area of vGlut1 positive puncta increased significantly, while the area of vGat positive puncta did not change. **F** Schematic depiction of this experiment. **G** Immunoblot analysis of synaptic protein levels in wild-type primary neurons treated with the conditioned medium of maternal VPA-treated neurons. Saline, Saline-treated neuron; VPA, VPA-treated neuron's medium. **H** Immunoblot quantification of synaptic protein levels in **B**) ($n = 5$, Mean ± SEM, Student's t-test, standardized by β3-tubulin). **I** Immunocytochemical analysis of vGlut1-, vGat-, and synaptophysin in wild-type primary neurons treated with the conditioned medium. Scale bar = 10 µm. **J**) Quantification of vGlut1- and vGat- positive presynapse areas in **I** ($n = 15$, MEAN ± SEM, One-way ANOVA was performed to assess the overall differences among groups. Post-hoc comparisons were conducted using Tukey's Honest Significant Differences (HST) test, standardized by synaptophysin).

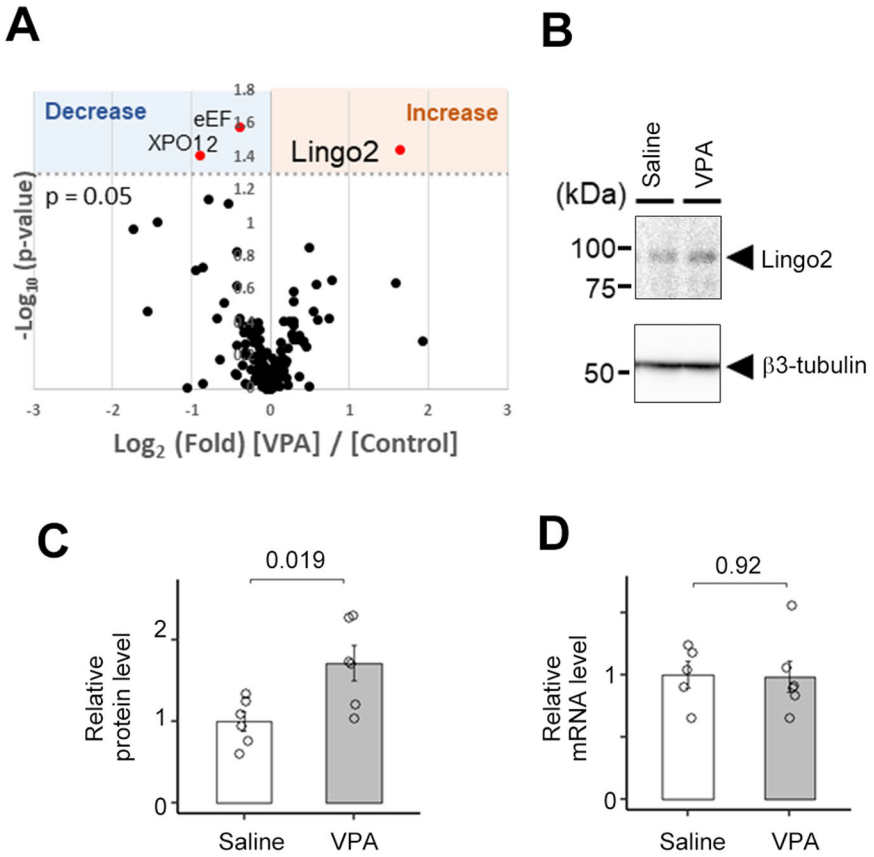

Fig. 2 Lingo2 expression level is increased in the Maternally VPA-treated neuron. A Volcano plot of the quantitative comparison between the secretomes of maternal VPA treated and Saline treated neurons of 3 experiments identified 145 proteins. Secretome proteins that are significantly changed are marked as red dots. Significantly changed protein: $p < 0.05$ (-log10 > 1.3). **B** Immunoblot analysis of mouse primary neurons obtained from maternal VPA-treated pups. **C** Quantification of Lingo2 protein level in **C** ($n = 6$, Mean ± SEM). Lingo2 protein level was increased in maternal VPA-treated neurons. **D** Quantification of Lingo2 mRNA level ($n = 5$, Mean ± SEM). Lingo2 mRNA level was unchanged in maternal VPA-treated neurons.

reaction on the beads. Using the SPECS method, several proteins were identified as substrate proteins for shedding proteases, such as BACE1 and ADAM10 [43, 44]. We used the SPECS method to comprehensively analyze the secretory proteins in CM-VPA. After comparison with the secretome of primary neurons derived from wild-type mice, we found that the levels of three candidate proteins were altered (Fig. 2A and supplementary table). Of these, leucine-rich repeat and immunoglobulin domain-containing protein 2 (Lingo2) were of particular interest. LINGO2 is a gene identified in the human chromosome 9p21.1 region as an ortholog of LINGO1 [48]. The role of LINGO2 in central nervous system functions is not well understood. In addition, copy number variations (CNVs) in the *LINGO2* gene have been reported in ASD patients, and genetic analysis using single-cell RNA sequencing data suggested that *LINGO2* expression correlates with the clinical severity of ASD [49–51]. We also confirmed increased protein expression of Lingo2 in the cell lysates of primary neurons derived from fetuses exposed to maternal VPA administration (Fig. 2B, C), although the mRNA levels of *Lingo2* were unaltered (Fig. 2D). These data suggest that the level of Lingo2 is regulated by protein metabolism in VPA-induced model neurons.

Lingo2 was cleaved by ADAM10 to secrete a soluble form of Lingo2

We identified peptides derived from Lingo2 in CM-VPA, although Lingo2 is a type 1 transmembrane protein. Therefore,

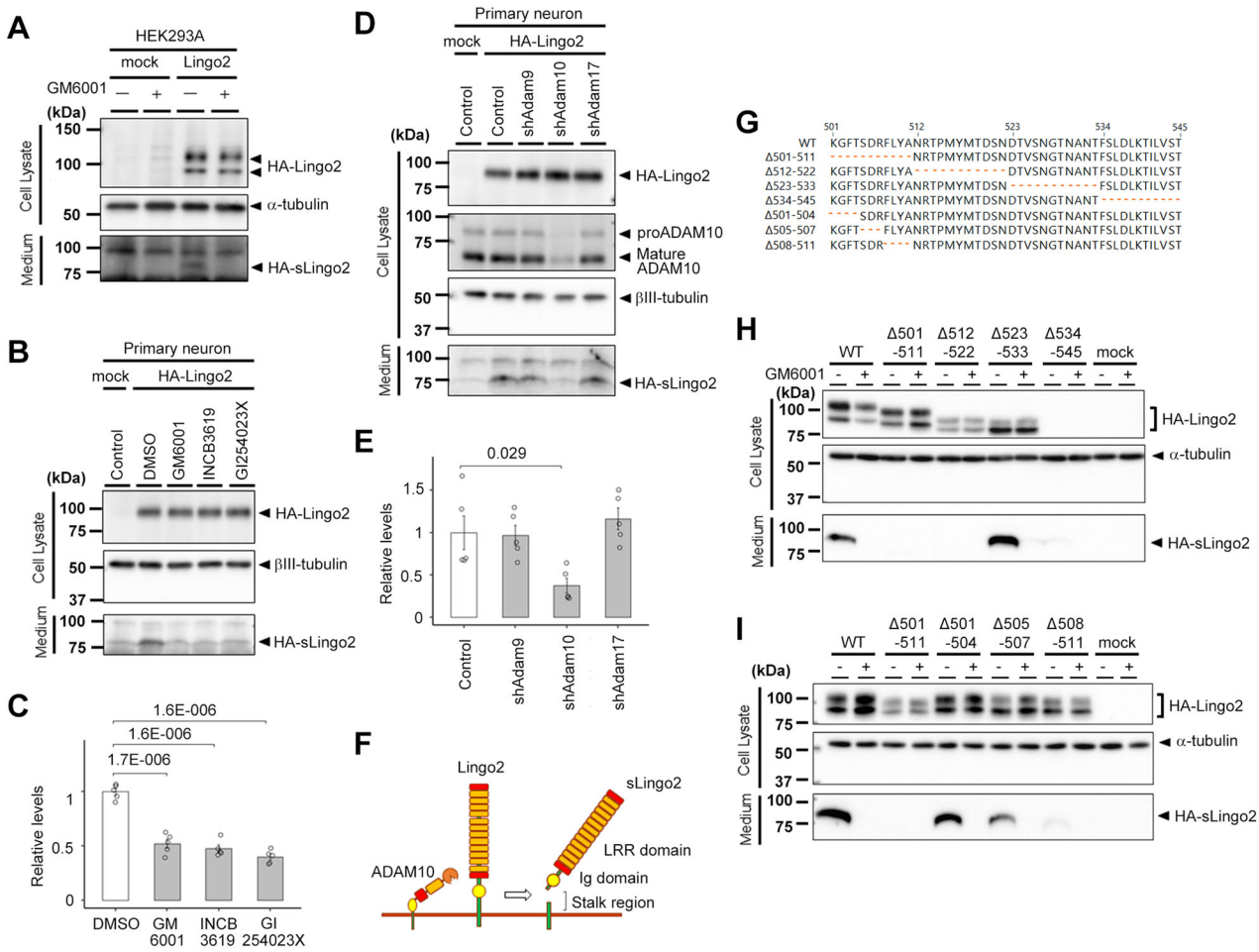

Fig. 3 Proteolytic processing of Lingo2. A Immunoblot analysis of the cell lysate and medium of the Lingo2 overexpressed HEK293A cells treated with or without metalloprotease inhibitor, GM6001. The soluble form of Ligno2 was diminished by the treatment of GM6001. **B** Immunoblot analysis of the cell lysate and medium of the Lingo2 overexpressed mouse primary neuron treated with or without metalloprotease inhibitory. **C** Quantification of sLingo2 protein level in mouse primary neurons. ($n = 5$, Mean ± SEM, One-way ANOVA was performed to assess the overall differences among groups. Post-hoc comparisons were conducted using Tukey's HST test). The soluble form of Ligno2 was diminished by the administration of GM6001, INCB,3619, and GI254023X. **D** Immunoblot analysis of the cell lysate and medium of the Lingo2 overexpressed and ADAM family knockdown mouse primary neurons. **E** Quantification of sLingo2 protein level in mouse primary neurons. ($n = 5$, Mean ± SEM, One-way ANOVA was performed to assess the overall differences among groups. Post-hoc comparisons were conducted using Tukey's HST test, $^*p < 0.05$). The soluble form of Lingo2 was diminished by knockdown of the ADAM10. **F** Schematic representation of Lingo2 and its processing. **G** Locations of deletion mutants at the stalk region of Lingo2. **H** Immunoblot analysis of the cell lysate and medium of the mutant Lingo2-expressing HEK293 cells. Note that no expression of Δ534-545 mutant was observed. **I** Immunoblot analysis of the cell lysate and medium of the mutant Lingo2-expressing HEK293 cells.

we hypothesized that it undergoes proteolytic processing to release the extracellular region into the conditioned medium. This metabolism is observed in other type 1 transmembrane proteins, such as APP and neuroligin [39, 52], which are cleaved at the juxtamembrane region by A disintegrin and metalloproteinase domain-containing proteins (ADAMs), releasing their extracellular domains. To study the protein metabolism of Lingo2, we overexpressed N-terminally HA-tagged Lingo2 in HEK 293A cells. The results showed that full-length HA-Lingo2 was detected as 95 and 110 kDa doublet bands in the cell lysates and a soluble form of HA-Lingo2 (sLingo2) of 80 kDa was found in the conditioned medium (Fig. 3A). The production of sLingo2 was reduced by the administration of GM6001, a broad-spectrum metalloproteinase inhibitor, suggesting that Lingo2 is cleaved by metalloproteinases to secrete sLingo2 (Fig. 3A). We also overexpressed HA-Lingo2 in primary mouse neurons and evaluated the effects of several metalloproteinase inhibitors; a broad-spectrum metalloproteinase inhibitor GM6001, the ADAM10 and ADAM17 inhibitor INCB3619 [39], and the ADAM10 inhibitor GI254023X [53]. sLingo2 production was abolished by all inhibitors (Fig. 3B – C), suggesting that Lingo2 is cleaved by ADAM10. To determine which ADAM is responsible for the cleavage of Lingo2, we generated shRNA lentiviral vectors targeting *Adam9*, *Adam10*, and *Adam17* and confirmed the reduction of the mRNA level of each ADAM protease. The amount of sLingo2 was abolished by *Adam10* knockdown, but not by *Adam9* or *Adam17* (Fig. 3D, E). Consistent with this, systematic proteomic analysis of *Adam10*-deficient neurons using SPECS also revealed that Lingo2 is one of the ADAM10 substrates [44]. Thus, these results suggest that ADAM10 cleaves Lingo2 in primary neurons (Fig. 3F).

ADAM10 cleaves its substrates at the juxtamembrane region [54]. Based on the molecular weight of sLingo2 and the enzymatic character of ADAM10, we hypothesized that Lingo2 is cleaved at the stalk region (i.e., 501-545 aa) located between the

immunoglobulin-like domain and the transmembrane domain. To narrow down the cleavage site, we systematically examined the proteolytic processing of HA-Lingo2 with deletion mutations at the stalk region (Fig. 3G) in HEK293A cells. HA-Lingo2 production was significantly reduced in the Δ501-511 and Δ512–522 mutants (Fig. 3H). Expression of the HA-Lingo2 was reduced by the deletion near the transmembrane domain (i.e., Δ534-545). We further generated microdeletion mutants at 501–511 and found that the Δ508–511 mutant failed to release HA-sLingo2 (Fig. 3I). Taken together, 508-522 aa at the stalk region of Lingo2 is critical for sLingo2 generation.

The soluble form of Lingo2 functions as the excitatory presynapses organizer in mouse primary neurons

To investigate the ability of sLingo2 to induce excitatory synaptogenesis, we tested the synaptogenic activity of recombinant HA-sLingo2-V5His purified from the conditioned medium of HA-sLingo2-V5His overexpressing HEK 293A cells (Fig. 4A). Treatment of primary mouse neurons with 10 nM HA-sLingo2-V5His resulted in a significant increase in the expression level of the excitatory presynaptic marker vGlut1 and no change in the expression level of the inhibitory presynaptic marker vGat (Fig. 4B, C). This effect was also confirmed by immunocytochemical analysis, which showed an increase in the area of vGlut1-positive presynaptic puncta and no change in the area of vGat-positive presynaptic puncta (Fig. 4D, E). To analyze the functional role of sLingo2, sLingo2 was administered to hippocampal slice cultures [46, 47], in which local-circuit synaptic interactions are preserved. Consistent with the result of primary cultures, treatment of 10 nM recombinant HA-sLingo2-V5His resulted in a significant increase in the expression level of vGlut1 (Fig. 4F, G). Next, to determine whether full-length Lingo2 can induce the formation of excitatory synapses, we co-cultured HEK293A cells overexpressing HA-Lingo2-V5His with primary cultured neurons and assessed their impact on excitatory synapse formation. However, no induction of excitatory synapses was observed on cells expressing HA-Lingo2-V5His (data not shown). These results indicate that sLingo2 selectively induces the formation of excitatory presynapses in mouse primary neurons.

Because the expression level of endogenous Lingo2 was increased in primary neurons derived from fetuses treated with VPA during pregnancy, we hypothesized that the knockdown of Lingo2 would correct the abnormal excitatory synaptogenesis in the VPA model. To investigate this, we performed Lingo2 knockdown using two Lingo2-targeting shRNAs. Immunoblot analysis showed that maternal administration of VPA significantly increased the expression of vGlut1, and Lingo2 knockdown attenuated this increase (Fig. 5A, B). The expression of vGat, however, remained unchanged. To further confirm these results, we analyzed the number of vGlut1-positive puncta, a measure of excitatory presynaptic formation, by immunocytochemistry on Lingo2 knockdown primary neurons expressing GFP. We found that the increased number of vGlut1-positive puncta induced by maternal administration of VPA was attenuated by Lingo2 knockdown (Fig. 5C, D). These results suggest that reducing the expression of Lingo2 can normalize excitatory presynaptic formation in the VPA model.

The soluble form of Lingo2 increased excitatory synapses in human iPSC-derived neurons

To explore the role of sLingo2 in human excitatory neurons, we examined its effects on human iPSC-derived neurons. We used a system that can induce differentiation into excitatory neurons in a short time (2 weeks) by overexpressing Neurogenin-2 [55]. The differentiated excitatory neurons expressed neuronal markers, including β3-tubulin (β3-tub), and excitatory post-synaptic marker proteins, including Homer1. After the iPSCs were fully differentiated into excitatory neurons, we administered purified sLingo2 (Fig. 6A) and confirmed a significant increase in the expression of Homer1, an excitatory postsynaptic marker (Fig. 6B, C), similar to that observed in primary mouse neurons. To quantify excitatory synaptogenesis, we stained for puncta co-staining with synapsin-1, a presynaptic marker, and Homer1, a postsynaptic marker, and counted the density of excitatory synapses on the dendritic marker Map2. Our results showed that sLingo2 treatment resulted in a significant increase in excitatory synaptic density (Fig. 6C), indicating that sLingo2 is capable of inducing excitatory synapses in human iPSC-derived excitatory neurons. To determine whether the increase in excitatory synapses induced by recombinant sLingo2 affected synaptic function, we measured miniature excitatory postsynaptic currents (mEPSCs) using the whole-cell patch-clamp method (Fig. 6D). Our results showed that recombinant sLingo2 administration significantly increased the frequency of mEPSCs without affecting the amplitude (Fig. 6E, F). Taken together, our data indicate that sLingo2 functions as an excitatory synapse organizer in human neurons.

DISCUSSION

This study identified that sLingo2, a proteolytic fragment of Lingo2 by ADAM10, functions as an excitatory synapse organizer in mouse and human neurons. sLingo2 is one of the plausible pathogenic molecules in the maternal VPA administration mouse model of ASD. Our results and previous genetic findings suggest that Lingo2 is a novel ASD-associated synaptic protein affecting the E/I ratio in neurons and is a potential therapeutic target.

SPECS analysis of conditioned medium from primary neurons derived from the VPA model revealed increased levels of sLingo2, which harbors the excitatory synapse organizer. Consistent with a previous report indicating Lingo2 as an ADAM10 substrate candidate, pharmacological and genetic approaches identified ADAM10 as the enzyme responsible for cleaving Lingo2 in primary neurons, similar to APP or neuroligins [39, 44, 54]. Importantly, the expression of endogenous full-length Lingo2 was significantly increased by VPA, which may function as an HDAC inhibitor. However, we did not observe the change in the level of Lingo2 mRNA, suggesting that the post-translational mechanism, such as stability and/or degradation, of Lingo2 protein, was affected by VPA. Further research on the metabolic system of Lingo2 would provide a more precise mechanism of the VPA-administered model. In the present study, Lingo2 was identified from the CM of primary cultured neurons derived from the cerebral cortex. However, Lingo2 is widely expressed in the hypothalamus, hippocampus, cerebral cortex, midbrain, and striatum, and may be involved in various functional abnormalities [56]. In addition, the physiological role(s) of Lingo2 in the central nervous system has not been described, and the receptor for sLingo2 has not been identified. Therefore, it is necessary to investigate Lingo2 function outside of the cerebral cortex as well as identify the signaling mechanism of sLingo2 at the molecular level in the future.

Through electrophysiological analysis, we also found that sLingo2 increased the frequency of mEPSCs without affecting the amplitude of mEPSCs in human iPSC-derived excitatory neurons. The frequency of mEPSCs is commonly used as an indicator of transmitter release at the presynaptic terminal, while the amplitude indicates receptor density and sensitivity at the postsynaptic membrane. Thus, the fact that only the frequency was increased after sLingo2 administration suggests a strong involvement of sLingo2 in presynaptic terminals. Our study showed that sLingo2 promotes excitatory synapse formation in both primary cultured mouse neurons and human iPSC-derived excitatory neurons, suggesting that Lingo2 plays a role in disrupting the E/I balance in the VPA model. However, it remains unclear whether the increase in sLingo2 induces ASD-like behavior in the animal model. Future studies will investigate whether in

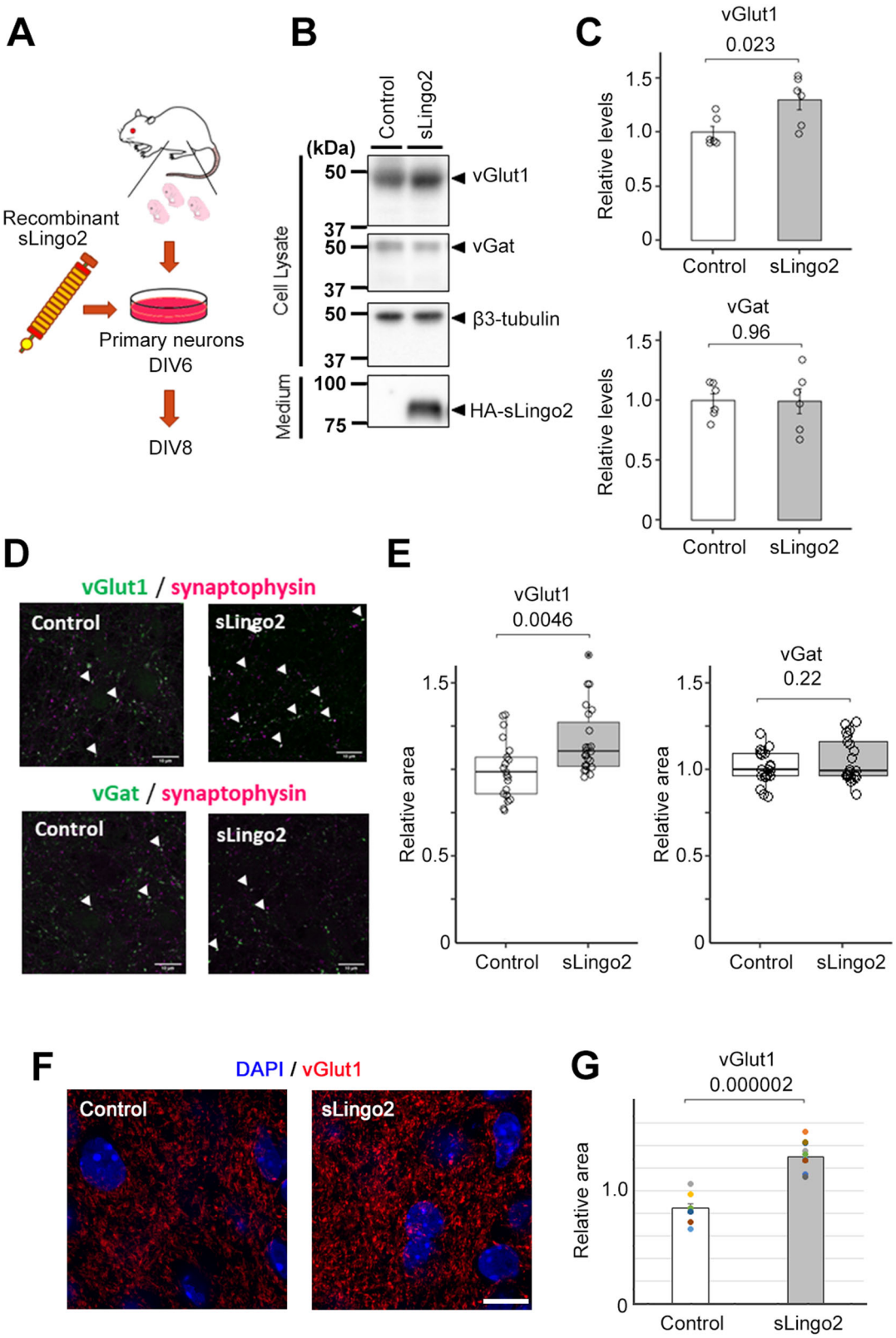

Fig. 4 Synaptic organizer activity of recombinant sLingo2. A Schematic depiction of this experiment. **B** Immunoblot analysis of synaptic protein level in primary neuron treated with the recombinant sLingo2. **C** Quantification of synaptic protein level in **B**) ($n = 6$, Mean ± SEM, Student's *t*-test, standardized by β3-tubulin). The expression of the vGlut was increased in sLingo2-treated neurons. **D** Immunocytochemical analysis of vGlut1, vGat, and synaptophysin in primary neurons treated with the sLingo2. Scale bar = 10 µm. **E** Quantification of vGlut1- and vGat-positive presynapse area in **D** ($n = 21$–23, Mean ± SEM, Student's t-test, standardized by synaptophysin). The relative vGlut1 puncta area was increased by the administration of the sLingo2, but the relative vGat puncta area did not change. **F** Immunohistochemical analysis of vGlut1 in hippocampal slice cultures treated with sLingo2. Scale bar = 10 µm. **G** Quantification of mean fluorescent intensity of vGlut1 in **F**) ($n = 8$ (control) and 10 (sLingo2) slices from 4, 3 mice each, Mean ± SEM, Student's *t*-test).

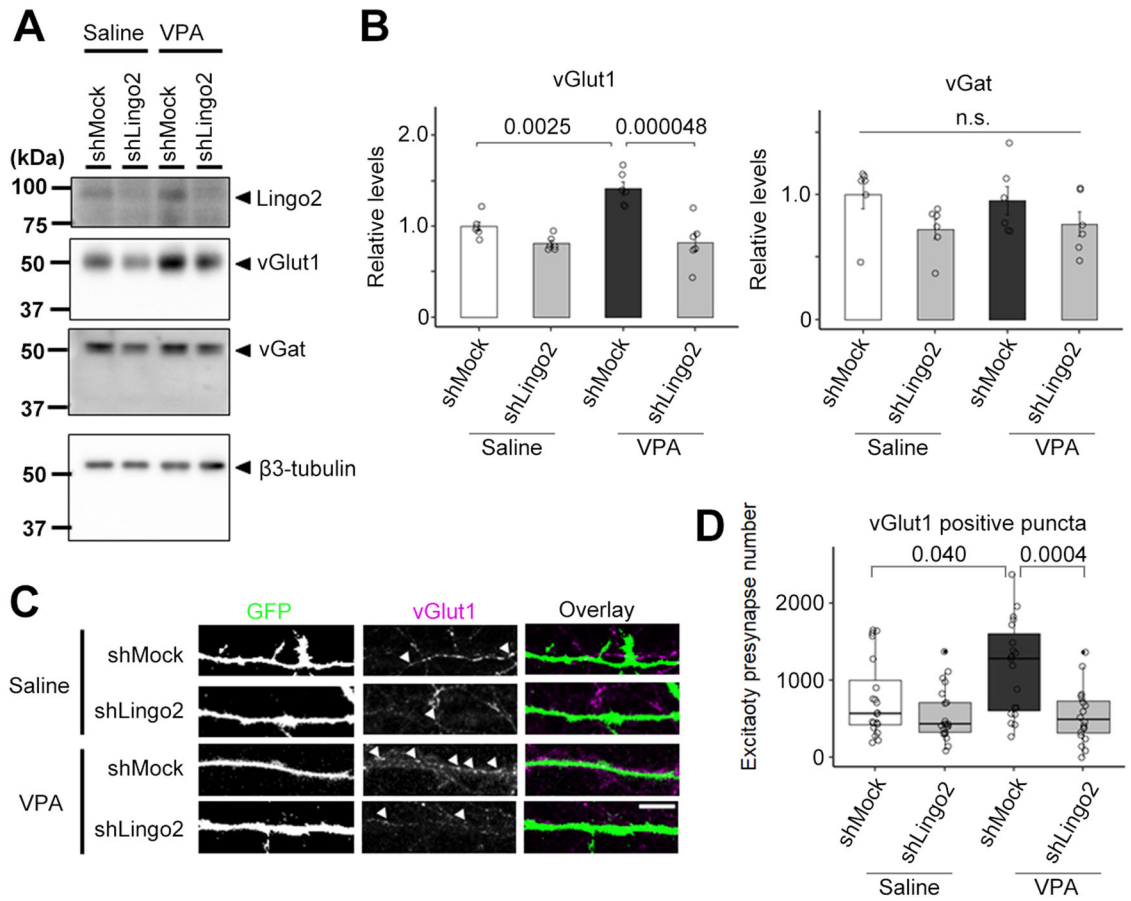

Fig. 5 Lingo2 is required for VPA-induced excitatory synapse formation. A Immunoblot analysis of synaptic protein level in *Lingo2* knockdown primary neuron from maternal VPA treated mouse. **B** Quantification of synaptic protein level in immunoblot ($n = 6$, Mean ± SEM, One-way ANOVA was performed to assess the overall differences among groups. Post-hoc comparisons were conducted using Tukey's HST test, standardized by β3-tubulin). The expression of the vGlut1 was increased in VPA-treated mice and decreased by *Lingo2* knockdown. **C** Immunocytochemical analysis of vGlut1 in *Lingo2* knockdown primary neuron from maternal VPA treated mouse. Scale bar = 10 µm. **D** Quantification of vGlut1-positive puncta number in **B** ($n = 20$, Mean ± SEM, One-way ANOVA was performed to assess the overall differences among groups. Post-hoc comparisons were conducted using Tukey's HST test. $^{*}p < 0.05$, $^{***}p < 0.001$). The number of the vGlut1 positive puncta was increased by VPA maternal administration and decreased by Lingo2 knockdown.

utero injection of sLingo2 protein or expression vector into the fetus can induce ASD-like behavior.

Several copy number variations (CNVs) of LINGO2 have been independently reported in individuals with ASD [49, 50]. In addition, analysis of RNA sequencing data from individuals with ASD has shown that the clinical severity of ASD correlates with LINGO2 expression [51]. These patient-based findings suggest that altered *LINGO2* expression may contribute to the development of ASD. The present study suggests that increased expression of Lingo2 in the VPA model is associated with an increase in sLingo2, disrupting the E/I balance. Interestingly, point mutations in NgR1, a potential receptor for sLingo2, have been reported in individuals with schizophrenia, suggesting that the LINGO2-NgR pathway may be involved in the development of neuropsychiatric disorders [57]. Further, we found that the stalk region of Lingo 2 is cleaved by ADAM10-mediated shedding. Notably, Δ523-533 mutant showed an increased production of sLingo2 (Fig. 3H), suggesting the possibility that mutations around the stalk region are associated with ASD by affecting the shedding of Lingo2. Mutation at the stalk region of TREM2 affects the risk of Alzheimer's by enhanced shedding of cell surface TREM2 [58, 59]. Thus, not only the total expression level but also SNPs/mutations and signaling mechanisms that affect Lingo2 metabolism may impact the ASD risk, which is an issue for future investigation.

This study suggests that abnormal levels of sLINGO2 in the brain may cause aberrant excitatory synaptogenesis and increase the risk of developing ASD. Knocking down Lingo2 expression to reverse the VPA-induced increase in excitatory synapses suggests that LINGO2 may be a potential target for the treatment of ASD. Although genetic studies support this idea, it is not known whether aberrant Lingo2 expression is associated with all ASD patients. Therefore, monitoring of LINGO2 and/or sLINGO2 expression levels would be required for the development of a LINGO2-targeted therapy. It is also anticipated that sLINGO2 levels in biological fluids may be used in the future as a biomarker for ASD. Following the diagnosis of LINGO2-related ASD, normalization of LINGO2 function/levels may be a viable therapeutic approach. Effective ways to inhibit sLINGO2 function include the use of neutralizing antibodies against sLINGO2 and/or blocking its receptor. Interventions targeting LINGO2-cleaving enzymes such as ADAM10 may also provide a novel therapeutic approach, although ADAM10 cleaves a variety of transmembrane proteins. In the future, it will be necessary to elucidate the detailed mechanism of excitatory synaptogenesis induced by sLINGO2 to identify more specific targets for intervention.

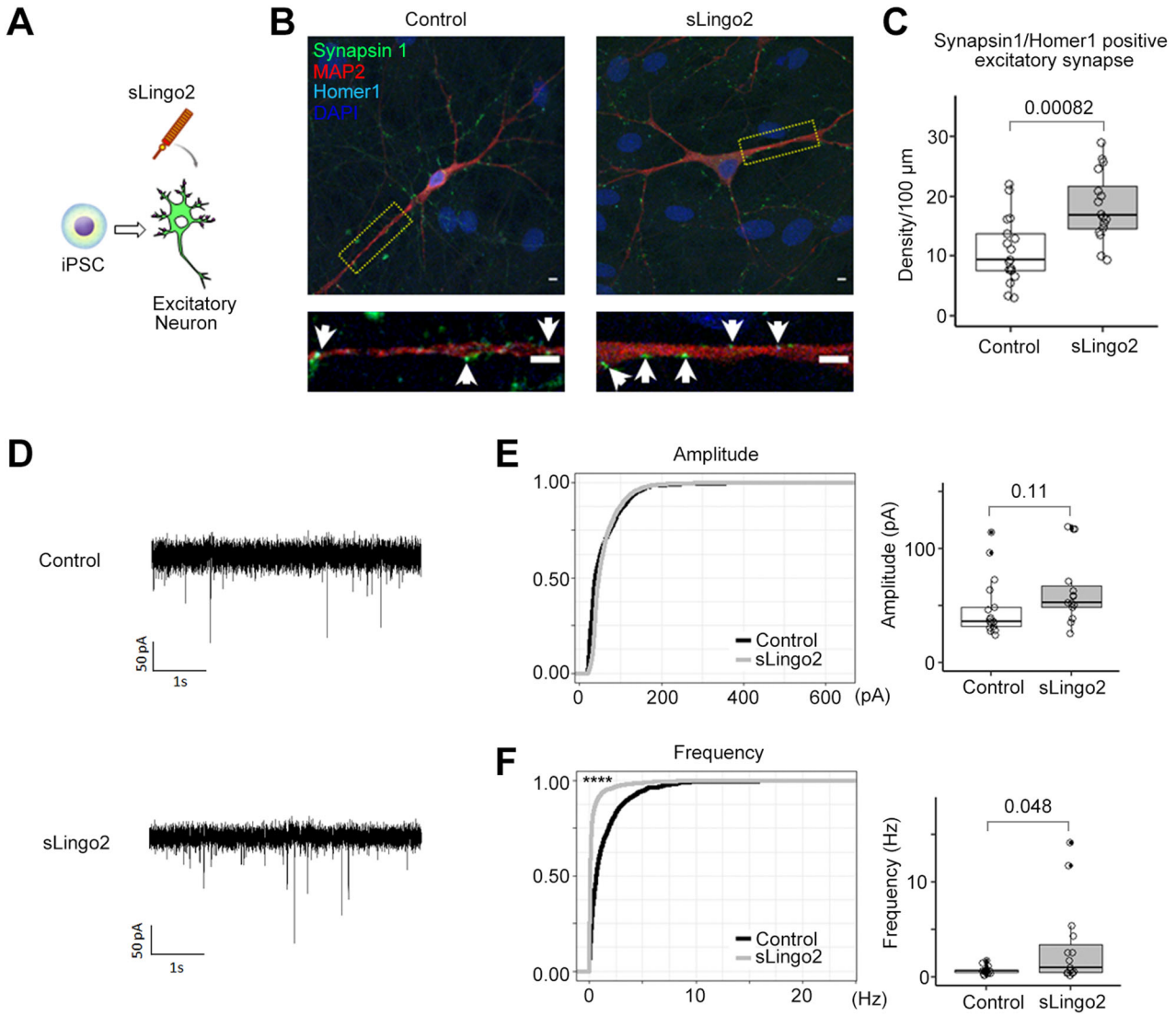

Fig. 6 Recombinant sLingo2 induces the excitatory synapse in human iPSC-derived neurons. A Schematic depiction of this experiment. **B** Immunocytochemical analysis in sLingo2 treated induced Excitatory neuron. Green: synapsin1, Red: Map2, Blue: DAPI, Cyan: Homer1, Scale bar = 10 µm **C** Quantification of synapsin1, homer1 double-positive puncta number in (**D**) ($n = 16–17$, Mean ± SEM, Student's *t*-test.). The double positive puncta number was increased with the administration of the sLingo2. **D** Representative mEPSC recordings from sLingo2 treated iPSC-derived excitatory neurons. **E** Cumulative probability of mEPSC amplitude and frequency. **F** Quantification of average mEPSC amplitude and frequency ($n = 15, 17$. Mean ± SEM. Student's *t*-test for average. Kolmogorov–Smirnov test for frequency. ****$p < 0.0001$). The average mEPSC frequency was increased with the administration of the sLingo2, while amplitude did not.

DATA AVAILABILITY

All data relevant to the study are included in the article or uploaded as online supplementary information. The data generated in this study will be available from the corresponding author upon reasonable request.

REFERENCES

1. Mattila ML, Kielinen M, Linna SL, Jussila K, Ebeling H, Bloigu R, et al. Autism spectrum disorders according to DSM-IV-TR and comparison with DSM-5 draft criteria: an epidemiological study. J Am Acad Child Adolesc Psychiatry. 2011;50:583–5.e11.
2. Saemundsen E, Magnússon P, Georgsdóttir I, Egilsson E, Rafnsson V. Prevalence of autism spectrum disorders in an Icelandic birth cohort. BMJ Open. 2013;3:e002748.
3. Kim YS, Leventhal BL, Koh YJ, Fombonne E, Laska E, Lim EC, et al. Prevalence of autism spectrum disorders in a total population sample. Am J Psychiatry. 2011;168:904–12.
4. Baron-Cohen S, Scott FJ, Allison C, Williams J, Bolton P, Matthews FE, et al. Prevalence of autism-spectrum conditions: UK school-based population study. Br J Psychiatry. 2009;194:500–9.
5. Idring S, Rai D, Dal H, Dalman C, Sturm H, Zander E, et al. Autism spectrum disorders in the Stockholm Youth Cohort: design, prevalence, and validity. PLoS One. 2012;7:e41280.
6. Russell G, Rodgers LR, Ukoumunne OC, Ford T. Prevalence of parent-reported ASD and ADHD in the UK: findings from the Millennium Cohort Study. J Autism Dev Disord. 2014;44:31–40.
7. Sun X, Allison C, Wei L, Matthews FE, Auyeung B, Wu YY, et al. Autism prevalence in China is comparable to Western prevalence. Mol Autism. 2019;10:7.
8. Rubenstein JLR, Merzenich MM. Model of autism: increased ratio of excitation/inhibition in key neural systems. Genes Brain Behav. 2003;2:255–67.
9. Mannion A, Leader G. Epilepsy in autism spectrum disorder. Res Autism Spectr Disord. 2014;8:354–61.
10. Cellot G, Cherubini E. GABAergic signaling as therapeutic target for autism spectrum disorders. Front Pediatr. 2014;2:70.
11. Yizhar O, Fenno LE, Prigge M, Schneider F, Davidson TJ, Ogshea DJ, et al. Neocortical excitation/inhibition balance in information processing and social dysfunction. Nature. 2011;477:171–8.
12. Gyulai L, Bowden CL, McElroy SL, Calabrese JR, Petty F, Swann AC, et al. Maintenance efficacy of divalproex in the prevention of bipolar depression. Neuropsychopharmacology. 2003;28:1374–82.

13. Phiel CJ, Zhang F, Huang EY, Guenther MG, Lazar MA, Klein PS. Histone deacetylase is a direct target of valproic acid, a potent anticonvulsant, mood stabilizer, and teratogen. J Biol Chem. 2001;276:36734–41.
14. Christensen J, Grnøborg TK, Srøensen MJ, Schendel D, Parner ET, Pedersen LH, et al. Prenatal valproate exposure and risk of autism spectrum disorders and childhood autism. JAMA. 2013;309:1696–703.
15. Bromley RL, Mawer GE, Briggs M, Cheyne C, Clayton-Smith J, García-Fiñana M, et al. The prevalence of neurodevelopmental disorders in children prenatally exposed to antiepileptic drugs. J Neurol Neurosurg Psychiatry. 2013;84:637–43.
16. Schneider T, Roman A, Basta-Kaim A, Kubera M, Budziszewska B, Schneider K, et al. Gender-specific behavioral and immunological alterations in an animal model of autism induced by prenatal exposure to valproic acid. Psychoneuroendocrinology. 2008;33:728–40.
17. Markram K, Rinaldi T, La Mendola D, Sandi C, Markram H. Abnormal fear conditioning and amygdala processing in an animal model of autism. Neuropsychopharmacology. 2008;33:901–12.
18. Roullet FI, Lai JKY, Foster JA. In utero exposure to valproic acid and autism–a current review of clinical and animal studies. Neurotoxicol Teratol. 2013;36:47–56.
19. Kim KC, Kim P, Go HS, Choi CS, Yang SI, Cheong JH, et al. The critical period of valproate exposure to induce autistic symptoms in Sprague-Dawley rats. Toxicol Lett. 2011;201:137–42.
20. Kataoka S, Takuma K, Hara Y, Maeda Y, Ago Y, Matsuda T. Autism-like behaviours with transient histone hyperacetylation in mice treated prenatally with valproic acid. Int J Neuropsychopharmacol. 2013;16:91–103.
21. Rasalam AD, Hailey H, Williams JHG, Moore SJ, Turnpenny PD, Lloyd DJ, et al. Characteristics of fetal anticonvulsant syndrome associated autistic disorder. Dev Med Child Neurol. 2005;47:551–5.
22. Rinaldi T, Kulangara K, Antoniello K, Markram H. Elevated NMDA receptor levels and enhanced postsynaptic long-term potentiation induced by prenatal exposure to valproic acid. Proc Natl Acad Sci USA. 2007;104:13501–6.
23. Lin HC, Gean PW, Wang CC, Chan YH, Chen PS. The amygdala excitatory/inhibitory balance in a valproate-induced rat autism model. PLoS One. 2013;8:e55248.
24. Traetta ME, Uccelli NA, Zárate SC, Gómez Cuautle D, Ramos AJ, Reinés A. Long-lasting changes in glial cells isolated from rats subjected to the valproic acid model of autism spectrum disorder. Front Pharmacol. 2021;12:707859.
25. Yang X, Tomita T, Wines-Samuelson M, Beglopoulos V, Tansey MG, Kopan R, et al. Notch1 signaling influences V2 interneuron and motor neuron development in the spinal cord. Dev Neurosci. 2006;28:102–17.
26. Iijima Y, Behr K, Iijima T, Biemans B, Bischofberger J, Scheiffele P. Distinct defects in synaptic differentiation of neocortical neurons in response to prenatal valproate exposure. Sci Rep. 2016;6:27400.
27. Yuzaki M. Two classes of secreted synaptic organizers in the central nervous system. Annu Rev Physiol. 2018;80:243–62.
28. Scheiffele P, Fan J, Choih J, Fetter R, Serafini T. Neuroligin expressed in nonneuronal cells triggers presynaptic development in contacting axons. Cell. 2000;101:657–69.
29. Gan KJ, Südhof TC. SPARCL1 promotes excitatory but not inhibitory synapse formation and function independent of neurexins and neuroligins. J Neurosci. 2020;40:8088–102.
30. Terauchi A, Johnson-Venkatesh EM, Toth AB, Javed D, Sutton MA, Umemori H. Distinct FGFs promote differentiation of excitatory and inhibitory synapses. Nature. 2010;465:783–7.
31. Martín-de-Saavedra MD, Dos Santos M, Culotta L, Varea O, Spielman BP, Parnell E, et al. Shed CNTNAP2 ectodomain is detectable in CSF and regulates Ca2+ homeostasis and network synchrony via PMCA2/ATP2B2. Neuron. 2022;110:627–.e9.
32. Tomita T, Maruyama K, Saido TCTC, Kume H, Shinozaki K, Tokuhiro S, et al. The presenilin 2 mutation (N141I) linked to familial Alzheimer disease (Volga German families) increases the secretion of amyloid β protein ending at the 42nd (or 43rd) residue. Proc Natl Acad Sci USA. 1997;94:2025–30.
33. Takasugi N, Tomita T, Hayashi I, Tsuruoka M, Niimura M, Takahashi Y, et al. The role of presenilin cofactors in the γ-secretase complex. Nature. 2003;422:438–41.
34. Araki M, Ito K, Takatori S, Ito G, Tomita T. BORCS6 is involved in the enlargement of lung lamellar bodies in Lrrk2 knockout mice. Hum Mol Genet. 2021;30:1618–31.
35. Kanatsu K, Morohashi Y, Suzuki M, Kuroda H, Watanabe T, Tomita T, et al. Decreased CALM expression reduces Aβ42 to total Aβ ratio through clathrin-mediated endocytosis of γ-secretase. Nat Commun. 2014;5:1–12.
36. Fukumoto H, Tomita T, Matsunaga H, Ishibashi Y, Saido TC, Iwatsubo T. Primary cultures of neuronal and non-neuronal rat brain cells secrete similar proportions of amyloid β peptides ending at Aβ40 and Aβ42. Neuroreport. 1999;10:2965–9.
37. Yumoto T, Kimura M, Nagatomo R, Sato T, Utsunomiya S, Aoki N, et al. Autism-associated variants of neuroligin 4X impair synaptogenic activity by various molecular mechanisms. Mol Autism. 2020;11:68.
38. Matsuzaki M, Yokoyama M, Yoshizawa Y, Kaneko N, Naito H, Kobayashi H, et al. ADAMTS4 is involved in the production of the Alzheimer disease amyloid biomarker APP669-711. Mol Psychiatry. 2023. https://doi.org/10.1038/S41380-023-01946-Y.
39. Suzuki K, Hayashi Y, Nakahara S, Kumazaki H, Prox J, Horiuchi K, et al. Activity-dependent proteolytic cleavage of neuroligin-1. Neuron. 2012;76:410–22.
40. Takahashi K, Tanabe K, Ohnuki M, Narita M, Ichisaka T, Tomoda K, et al. Induction of Pluripotent stem cells from adult human fibroblasts by defined factors. Cell. 2007;131:861–72.
41. Nakagawa M, Taniguchi Y, Senda S, Takizawa N, Ichisaka T, Asano K, et al. A novel efficient feeder-Free culture system for the derivation of human induced pluripotent stem cells. Sci Rep. 2014;4:3594.
42. Oceguera-Yanez F, Kim SI, Matsumoto T, Tan GW, Xiang L, Hatani T, et al. Engineering the AAVS1 locus for consistent and scalable transgene expression in human iPSCs and their differentiated derivatives. Methods. 2016;101:43–55.
43. Kuhn PH, Koroniak K, Hogl S, Colombo A, Zeitschel U, Willem M, et al. Secretome protein enrichment identifies physiological BACE1 protease substrates in neurons. EMBO J. 2012;31:3157–68.
44. Kuhn P-H, Colombo AV, Schusser B, Dreymueller D, Wetzel S, Schepers U, et al. Systematic substrate identification indicates a central role for the metalloprotease ADAM10 in axon targeting and synapse function. Elife. 2016;5:e12748.
45. Shevchenko A, Wilm M, Vorm O, Mann M. Mass spectrometric sequencing of proteins silver-stained polyacrylamide gels. Anal Chem. 1996;68:850–8.
46. Kasahara Y, Koyama R, Ikegaya Y. Depth and time-dependent heterogeneity of microglia in mouse hippocampal slice cultures. Neurosci Res. 2016;111:64–69.
47. Koyama R, Muramatsu R, Sasaki T, Kimura R, Ueyama C, Tamura M, et al. A Low-cost method for brain slice cultures. J Pharmacol Sci. 2007;104:191–4.
48. Carim-Todd L, Escarceller M, Estivill X, Sumoy L. LRRN6A/LERN1 (leucine-rich repeat neuronal protein 1), a novel gene with enriched expression in limbic system and neocortex. Eur J Neurosci. 2003;18:3167–82.
49. Matsunami N, Hadley D, Hensel CH, Christensen GB, Kim C, Frackelton E, et al. Identification of rare recurrent copy number variants in high-risk autism families and their prevalence in a large ASD population. PLoS One. 2013;8:e52239.
50. Gazzellone MJ, Zhou X, Lionel AC, Uddin M, Thiruvahindrapuram B, Liang S, et al. Copy number variation in Han Chinese individuals with autism spectrum disorder. J Neurodev Disord. 2014;6:34.
51. Ji G, Li S, Ye L, Guan J. Gene module analysis reveals cell-type specificity and potential target genes in autism's pathogenesis. Biomedicines. 2021;9:410.
52. Kikuchi K, Kidana K, Tatebe T, Tomita T. Dysregulated metabolism of the Amyloid-β protein and therapeutic approaches in Alzheimer disease. J Cell Biochem. 2017;118:4183–90.
53. Hundhausen C, Misztela D, Berkhout TA, Broadway N, Saftig P, Reiss K, et al. The disintegrin-like metalloproteinase ADAM10 is involved in constitutive cleavage of CX3CL1 (fractalkine) and regulates CX3CL1-mediated cell-cell adhesion. Blood. 2003;102:1186–95.
54. Saftig P, Lichtenthaler SF. The alpha secretase ADAM10: A metalloprotease with multiple functions in the brain. Prog Neurobiol. 2015;135:1–20.
55. Zhang Y, Pak CH, Han Y, Ahlenius H, Zhang Z, Chanda S, et al. Rapid single-step induction of functional neurons from human pluripotent stem cells. Neuron. 2013;78:785–98.
56. Guillemain A, Laouarem Y, Cobret L, Štefok D, Chen W, Bloch S, et al. LINGO family receptors are differentially expressed in the mouse brain and form native multimeric complexes. FASEB J. 2020;34:13641–53.
57. Kimura H, Fujita Y, Kawabata T, Ishizuka K, Wang C, Iwayama Y, et al. A novel rare variant R292H in RTN4R affects growth cone formation and possibly contributes to schizophrenia susceptibility. Transl Psychiatry. 2017;7:e1214.
58. Schlepckow K, Kleinberger G, Fukumori A, Feederle R, Lichtenthaler SF, Steiner H, et al. An Alzheimer-associated TREM2 variant occurs at the ADAM cleavage site and affects shedding and phagocytic function. EMBO Mol Med. 2017;9:1356–65.
59. Thornton P, Sevalle J, Deery MJ, Fraser G, Zhou Y, Ståhl S, et al. TREM2 shedding by cleavage at the H157-S158 bond is accelerated for the Alzheimer's disease-associated H157Y variant. EMBO Mol Med. 2017;9:1366–78.

ACKNOWLEDGEMENTS

The authors are grateful to Drs. Tohru Fukuyama, Satoshi Yokoshima (Nagoya University), and Motoji Kitaura (Shionogi & Co. Ltd.) for valuable reagents, and our current and previous laboratory members for helpful discussions. This work was supported in part by Shionogi & Co. Ltd. (to T.T.), Daiichi Sankyo Foundation of Life Science (to T.T.), a Grant-in-Aid for Scientific Research (A) (15H02492, 19H01015, 23H00394 to T.T.), Challenging Research (Exploratory) (20K21471 to T.T.), Scientific Research (22K21353 to Y.I.) from the Japan Society for the Promotion of Science (JSPS), The Institute for AI and Beyond of the University of Tokyo (to Y.I.), JST ERATO (JPMJER1801 to Y.I.), AMED CREST (22g1510002h0002 to Y.I.), the Deutsche Forschungsgemeinschaft (DFG, German Research Foundation) under Germany's

Excellence Strategy within the framework of the Munich Cluster for Systems Neurology (EXC2145 SyNergy– ID390857198 to S.F.L.) and World-leading Innovative Graduate Study Program for Life Science and Technology from the University of Tokyo (to F.Y.). M.K. receives a research fellowship for young scientists from JSPS (19J14908).

AUTHOR CONTRIBUTIONS

F.Y., R.N., and T.T. conceived and designed the study. F.Y., R.N., M.K., S.S., Y.K., Y.N., S.F.L., S.T., and G.I. performed the molecular biological and biochemical experiments and analyzed the data. F.Y., S.U., K.M., H.T., and K.O., performed the electrophysiological experiments and analyzed the data. R.Kono, R.Koyama, Y.I., performed the slice culture experiments and analyzed the data. All authors contributed to the interpretation of the results. F.Y. drafted the first version of the manuscript. T.T. reviewed and edited the manuscript. All authors provided critical comments and approved the final version of the manuscript.

COMPETING INTERESTS

S.U., M.K., K.T., K.M., and H.T. were full-time employees of Shionogi & Co., Ltd., Japan. The authors have no other conflicts of interest in association with this manuscript.

ADDITIONAL INFORMATION

Supplementary information The online version contains supplementary material available at https://doi.org/10.1038/s41398-024-03167-5.

Correspondence and requests for materials should be addressed to Taisuke Tomita.